Mixed Conductivity of Zircon-Type $Ce_{1-x}A_xVO_{4\pm\delta}$ (A = Ca, Sr)

E.V. Tsipis[a], V.V. Kharton[a,b*], N.P. Vyshatko[a], A.L. Shaula[a], M.V. Patrakeev[a,c] and J.R. Frade[a]

[a]Department of Ceramics and Glass Engineering, CICECO, University of Aveiro, 3810-193 Aveiro, Portugal

[b]Inst. of Physicochemical Problems, Belarus State Univ., 14 Leningradskaya Str., 220050 Minsk, Rep. of Belarus

[c]Institute of Solid State Chemistry, Ural Division of RAS, 91 Pervomaiskaya Str., Ekaterinburg 620219, Russia

Abstract. Incorporation of alkaline-earth cations into the zircon-type lattice of $Ce_{1-x}A_xVO_{4+\delta}$ (A = Ca, Sr; x = 0 – 0.2) was found to significantly increase the p-type electronic conductivity and to decrease the Seebeck coefficient, which becomes negative at $x \geq 0.1$. The oxygen ionic conductivity is essentially unaffected by doping. The ion transference numbers of $Ce_{1-x}A_xVO_{4+\delta}$ in air, determined by the faradaic efficiency measurements, are in the range from 2×10^{-4} to 6×10^{-3} at 973-1223 K, increasing when temperature increases or alkaline-earth cation content decreases. The results on the partial conductivities and Seebeck coefficient suggest the presence of hyperstoichiometric oxygen, responsible for ionic transport, in the lattice of doped cerium vanadates. The activation energies for the electron-hole and ionic conduction both decrease on doping and vary in the ranges 39-45 kJ/mol and 87-112 kJ/mol, respectively.

1. Introduction

Phases derived from cerium orthovanadate, $CeVO_4$, attract a significant interest due to their unique optical, catalytic and electrical properties, suggesting potential applications as counter electrodes in electrochromic devices, oxidation catalysts and luminescent materials [1-8]. The compound $CeVO_4$, having a tetragonal zircon-type structure (space group $I4_1/amd$), is one of exceptional examples where Ce^{3+} cations are stabilized in oxidizing conditions, particularly in air. The dominant trivalent state of cerium ions was confirmed by X-ray absorption spectroscopy (XAS) and thermogravimetric analysis (TGA) [7,9]. These data cannot however exclude a presence of minor fractions of Ce^{4+}, supposed in Ref. [5].

The total conductivity of undoped cerium orthovanadate is predominantly p-type electronic, with activation energy of approximately 0.37 eV at 380-995 K [7]. At 400-680 K, the electron-hole transport was assumed to occur via the hopping between Ce^{4+} and Ce^{3+} ions [5]. Substitution of cerium with lower-valence cations, particularly calcium and strontium, considerably increases total conductivity. The highest values of the conductivity in air were reported for the compositions $Ce_{0.8}Ca_{0.2}VO_4$ and $Ce_{0.9}Sr_{0.1}VO_4$ [7]. The oxygen ionic transference numbers of $CeVO_4$ and $Ce_{1-x}A_xVO_4$ (A = Ca, Sr, Pb), evaluated by the e.m.f. method at temperatures up to 1073 K, were found lower than the detection limit [7].

As $CeVO_4$-based phases possess a high catalytic activity [4] combined with a significant total conductivity [7], these materials may be of interest for high-temperature electrochemical applications, provided that they meet the requirements on phase stability and ionic transport under the operation conditions. The present work is centered on the study of partial oxygen ionic and p-type electronic conductivities of $Ce_{1-x}A_xVO_4$ (A = Ca, Sr; x = 0 - 0.2) in atmospheric air.

*Corresponding author. Present address: Department of Ceramics and Glass Engineering, CICECO, University of Aveiro, 3810-193 Aveiro, Portugal. Fax: +351-234-425300; Tel.: +351-234-370263; E-mail: kharton@cv.ua.pt

2. Experimental Description

Single-phase powders of $CeVO_4$, $Ce_{0.9}Sr_{0.1}VO_4$ and $Ce_{1-x}Ca_xVO_4$ (x = 0.1 and 0.2) were synthesized by a standard ceramic route from the stoichiometric amounts of high-purity $Ce(NO_3)_3{\cdot}6H_2O$, V_2O_5, $SrCO_3$ and $CaCO_3$. The reactions were conducted at 823 - 1123 K for 10-30 hours in air. Formation of single zircon-type phases was confirmed by X-ray diffraction (XRD) analysis. Gas-tight ceramics were obtained from the ball-milled powders, compacted at 200-350 MPa into the disks (diameter of 10-15 mm) and then sintered at 1420 – 1650 K during 2 - 8 hours with subsequent slow cooling, in order to achieve equilibrium with air at low temperatures. Characterization of the ceramic materials involved XRD, scanning electron microscopy combined with energy dispersive spectroscopy (SEM/EDS), and thermogravimetric and differential thermal analysis (TGA/DTA). The total electrical conductivity in air was measured at 373-1223 K by 4-probe DC technique, van der Pauw method and AC impedance spectroscopy. The measurements of Seebeck coefficient (α) were performed at 1023-1223 K in air. The experimental techniques and equipment used for the general characterization and electrical measurements can be found elsewhere (Refs. [10-16] and references cited).

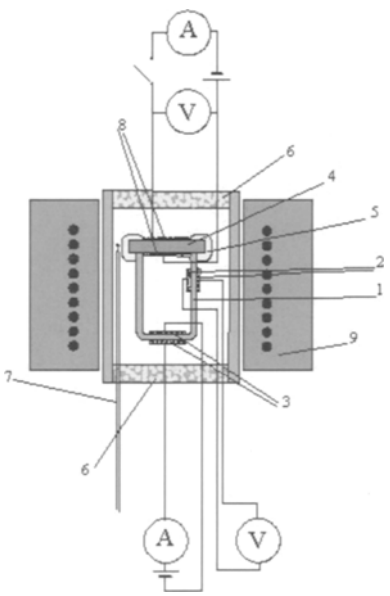

Fig. 1. Schematic drawing of the electrochemical cell for faradaic efficiency measurements: (1), YSZ electrolyte, (2), electrodes of the oxygen sensor, (3), electrodes of the oxygen pump, (4), sample under test, (5), high-temperature sealant, (6), porous ceramic insertions, (7), thermocouple, (8), Pt electrodes applied onto the specimen, (9), furnace.

The values of the oxygen ion transference numbers (t_o) and ionic conductivity (σ_o) were calculated from the results of faradaic efficiency measurements, carried out at 973-1223 K under zero oxygen chemical potential gradient in atmospheric air. The measuring cells comprised an oxygen pump and a sensor made of yttria-stabilized zirconia (YSZ) solid-electrolyte. After sealing of a gas-tight ceramic sample with porous Pt electrodes onto the zirconia cell (Fig. 1), a direct current I_{in} was passed through the sample pumping oxygen into the cell, and a current I_{out} was simultaneously passed through the pump, removing oxygen from the cell. The time-independent current values were adjusted to provide sensor e.m.f. values to be constant and close to zero:

$$E = \frac{RT}{4F} \ln\left(\frac{p_2}{p_1}\right) \approx 0 \qquad (1)$$

where p_1 and p_2 were the oxygen partial pressures inside and outside the cell. In steady-state conditions, oxygen chemical potential gradients across the membrane were therefore negligible. As the steady oxygen fluxes through the sample (J_{in}) and pump (J_{out}) should be equal

$$J_{in} = J_{out} = I_{out}{\cdot}(4F)^{-1} = t_o{\cdot}I_{in}{\cdot}(4F)^{-1} \qquad (2)$$

Respectively, the oxygen ion transference number can be determined as

$$t_o = I_{out} / I_{in} \qquad (3)$$

Each t_o value presented in this paper was averaged from 2-4 experimental data points.

3. Results and Discussion

XRD and SEM/EDS analyses detected no secondary phases in the sintered $Ce_{1-x}A_xVO_4$ ceramics. One example of X-ray diffraction pattern for undoped $CeVO_4$ at room temperature is given in Fig. 2A. No phase changes were found at temperatures up to 1223 K in air by high-temperature XRD and the analysis of quenched samples (Fig. 2B), though a transition of the zircon- to scheelite-type phase of $CeVO_4$ around 1173 K was suggested in Ref. [5]. DTA confirmed literature data [5] on the presence of an endothermal effect in the high-temperature range. However, for all studied compositions, XRD results show that the zircon-type phases are stable in oxidizing conditions, at least, up to 1223-1273 K. Further heating leads to a segregation of CeO_2 phase, which is associated, most probably, with formation of A-site defi-

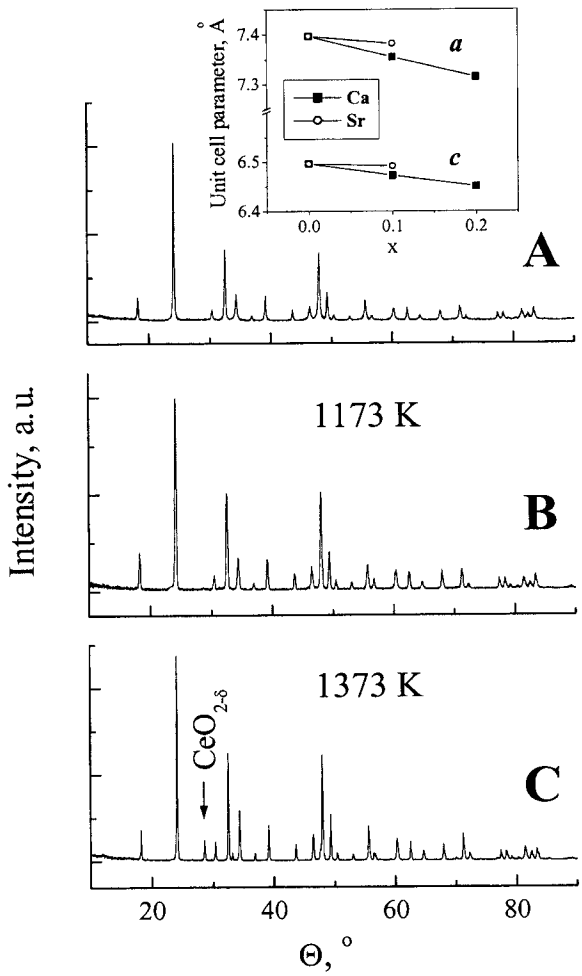

Fig. 2. XRD patterns of $CeVO_4$ ceramic samples: as-sintered and slowly cooled (A), quenched from 1173 K (B) and 1373 K (C). Inset shows composition dependencies of the tetragonal unit cell parameters of zircon-type $Ce_{1-x}A_xVO_4$.

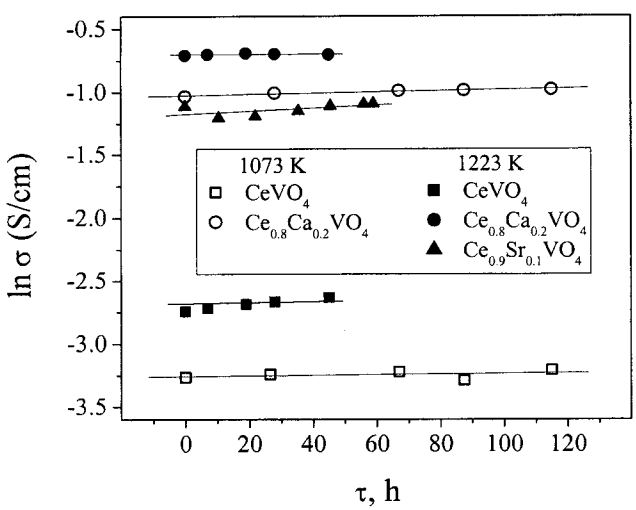

Fig. 3. Time dependence of the total conductivity of $Ce_{1-x}A_xVO_4$ ceramics in air.

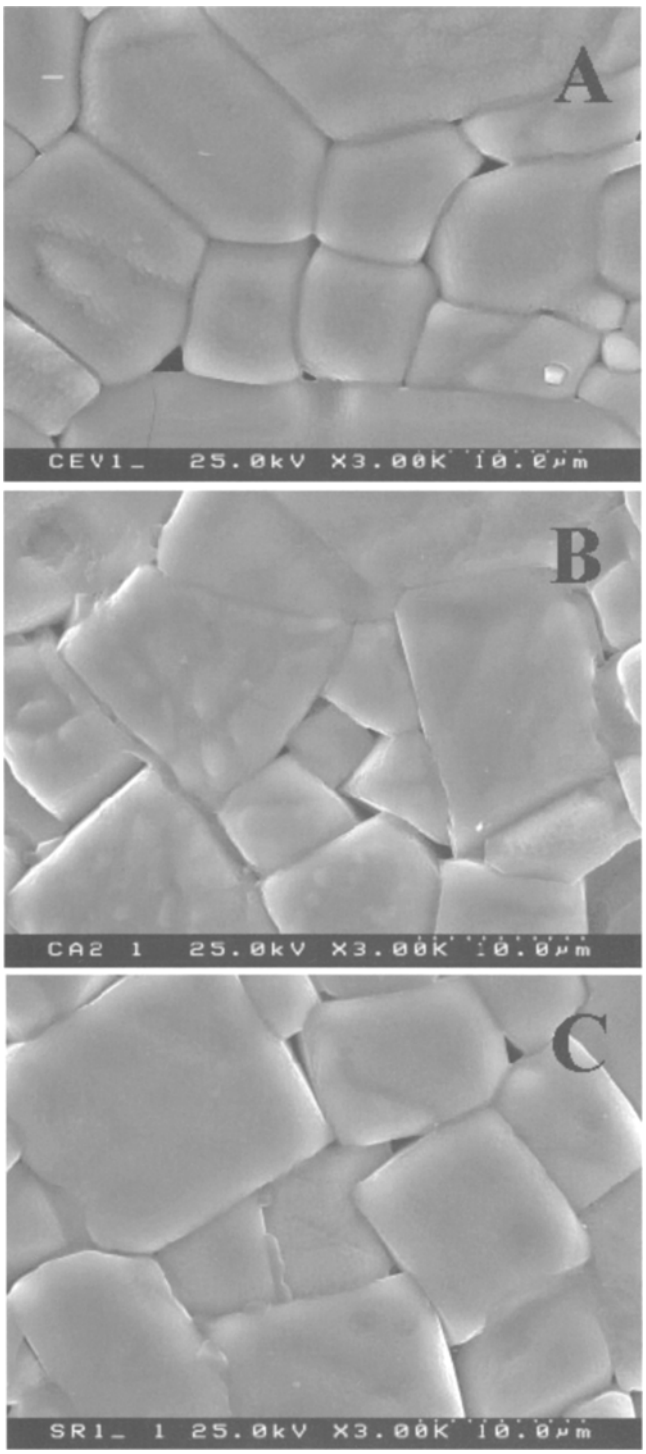

Fig. 4. SEM micrographs of polished and thermally etched ceramics: $CeVO_4$ (A), $Ce_{0.8}Ca_{0.2}VO_4$ (B), and $Ce_{0.9}Sr_{0.1}VO_4$ (C).

cient cerium vanadates. A similar behavior was observed on the reduction of zircon-type phases in vacuum. As an example, Fig. 2C presents XRD pattern of cerium vanadate ceramics, annealed at 1373 K in air and quenched in liquid

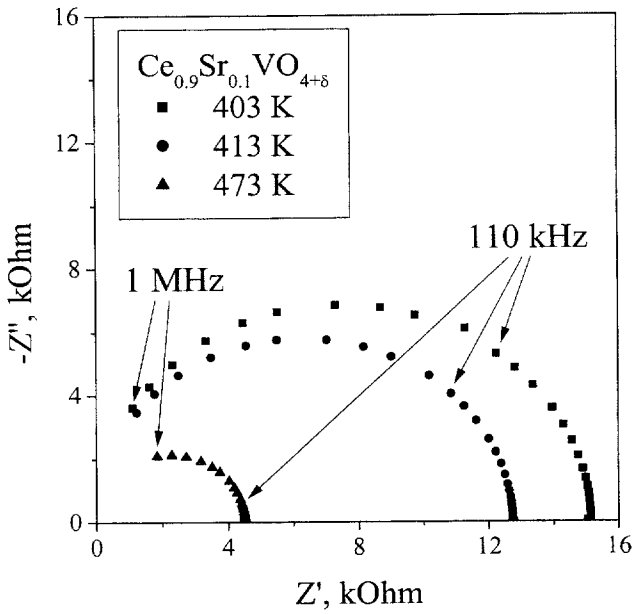

Fig. 5. Examples of typical impedance spectra of $Ce_{0.9}Sr_{0.1}VO_4$ ceramics.

nitrogen, where the amount of segregated CeO_2 is approximately 30%. Detailed studies of the decomposition mechanism and evaluation of the stability limits of $CeVO_4$-based phases are now in progress.

Taking into account that phase decomposition of zircon-type $Ce_{1-x}A_xVO_4$ may lead to a time degradation of the ionic and/or electronic transport, stability tests of the total conductivity and faradaic efficiency were carried out. Selected examples on the conductivity in air are shown in Fig. 3. At 973-1223 K, the transport properties of cerium vanadate-based ceramics were found to be essentially time-independent, which suggests an absence of phase changes, in agreement with XRD results. Therefore, one can assume that the data on ionic conductivity presented below are related to single zircon-type phases.

SEM micrographs reflecting characteristic microstructures of $Ce_{1-x}A_xVO_4$ are presented in Fig. 4. The average grain size was similar for all materials, varying in the range 7-20 μm. The density of the ceramic materials was higher than 93% of theoretical. EDS analysis confirmed that, within the limits of experimental error, the cation composition is uniform, in spite of liquid phase formation observed at the grain boundaries of thermally etched samples. Figures 4B and 4C indicate that liquid phase forms mainly in Ca– or Sr-containing samples. However, impedance spectra suggested a single contribution, even at relatively low temperatures (Fig. 5). Typical values of capacitance are in the range 10 pF to 50 pF, which are in the range expected for a bulk (intragrain) contribution, and

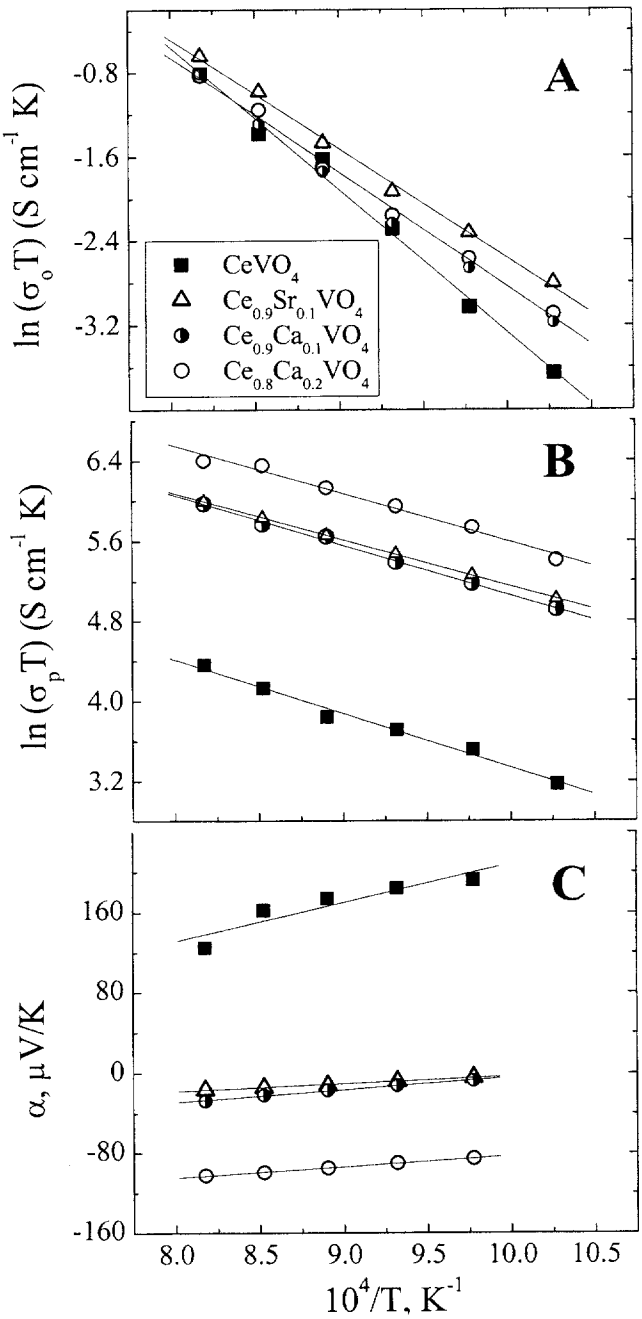

Fig. 6. Temperature dependence of the oxygen ionic (A) and p-type electronic (B) conductivities and Seebeck coefficient (C) of $Ce_{1-x}A_xVO_{4+\delta}$ ceramics in air.

order of magnitude below the values expected for internal interfaces. Moreover, the total conductivity values obtained by different techniques, including 4-probe DC and van der Pauw methods and the AC impedance spectroscopy, were found to be equal within the limits of experimental uncertainty and very similar to literature data [7]. Nevertheless, the overall trend is essentially due to the main conductivity contribution, which is, as discussed below, p-type electronic; one cannot exclude the possibility of significant grain

Table 1. Parameters of the oxygen ion transport in $Ce_{1-x}A_xVO_{4+\delta}$ in air.

Composition T, K	$CeVO_{4+\delta}$	$Ce_{0.9}Ca_{0.1}VO_{4+\delta}$	$Ce_{0.8}Ca_{0.2}VO_{4+\delta}$	$Ce_{0.9}Sr_{0.1}VO_{4+\delta}$
	Average ion transference numbers, t_o			
1223	5.6×10^{-3}	1.1×10^{-3}	7.3×10^{-4}	1.3×10^{-3}
1173	4.1×10^{-3}	8.6×10^{-4}	5.5×10^{-4}	1.1×10^{-3}
1123	4.2×10^{-3}	6.2×10^{-4}	3.9×10^{-4}	8.0×10^{-4}
1073	2.5×10^{-3}	4.9×10^{-4}	3.0×10^{-4}	6.1×10^{-4}
1023	1.4×10^{-3}	3.9×10^{-4}	2.5×10^{-4}	5.1×10^{-4}
973	1.1×10^{-3}	3.1×10^{-4}	2.0×10^{-4}	4.0×10^{-4}
	Activation energy for the ionic and electronic conductivities* (973 – 1223 K), kJ/mol			
$E_a(\sigma_o)$	112±14	93±8	91±9	87±7
$E_a(\sigma_p)$	45±7	42±3	40±7	39±1

* The oxygen ionic and p-type electronic conductivity was calculated from the results on the total conductivity and transference numbers, determined by the faradaic efficiency method.

boundary blocking effects on a minor ionic conductivity contribution.

The measurements of faradaic efficiency showed that the ionic contribution to total conductivity of the title materials is minor. The oxygen ion transference numbers of $Ce_{1-x}A_xVO_4$ vary in the range from 2×10^{-4} to 6×10^{-3} at 973-1223 K in air, increasing with temperature and decreasing when alkaline-earth dopant concentration increases (Table 1). The temperature dependencies of the partial oxygen ionic and electronic conductivities, derived from the results of faradaic efficiency and total conductivity measurements in air, are presented in Figs. 6A and 6B, respectively. The values of the activation energy (E_a) were calculated by the standard Arrhenius equation

$$\sigma = \frac{A_o}{T} \exp\left[-\frac{E_a}{RT}\right] \quad (4)$$

where A_0 is the pre-exponential factor. The activation energies for the ionic and electronic conduction are in the ranges 87-112 kJ/mol and 39-45 kJ/mol, respectively (Table 1). In both cases, E_a values were found to decrease with increasing dopant concentration.

Although at temperatures below 1100 K ionic conductivity of pure cerium vanadate is slightly lower than that of Ca-containing compositions, the values of σ_o are quite similar for all studied materials, being dependent on the type of dopant cations rather than on their concentration (Fig. 6A); this can be interpreted in terms of a dominant interstitial migration mechanism, related to hyper-stoichiometric oxygen in the lattice. Though this finding is not compelling evidence, the structure refinement and electron-hole concentration calculations [15] also suggest significant oxygen excess. Some authors [7-9] assumed cerium vanadate phase to be nearly oxygen-stoichiometric, with a prevailing charge compensation mechanism via the oxygen vacancy formation. In this case, however, a systematic increase in the ionic conduction with Ca content should be expected due to increasing oxygen vacancy concentration, which is not observed experimentally. On the other hand, a coexistence of oxygen vacancies and interstitials with an intrinsic Frenkel-type equilibrium in the $Ce_{1-x}Ca_xVO_{4+\delta}$ lattice, like in $La_2NiO_{4+\delta}$-based phases [16], cannot be entirely excluded. Another necessary comment is that the higher ionic conductivity of $Ce_{0.9}Sr_{0.1}VO_{4+\delta}$ in comparison with $Ce_{1-x}Ca_xVO_{4+\delta}$ (x = 0 – 0.2) seems to be analogous to the behavior of perovskite-type materials, where the ionic transport increases with increasing A-site cation radius (see [16] and references cited).

Contrary to the oxygen ionic conduction, the values of electronic conductivity are determined by the acceptor dopant concentration and are almost independent of the type of A-site substituent (Fig. 6B). In particular, $Ce_{0.9}Ca_{0.1}VO_{4+\delta}$ and $Ce_{0.9}Sr_{0.1}VO_{4+\delta}$ exhibit similar level of electron-hole transport. This behavior suggests the charge compensation mechanism via the formation of holes located, most likely, on cerium cations, which has no essential effect on the anion charge carrier concentration. In combination with the

negative slope of α - T dependencies (Fig. 6C), the systematic increase in the conductivity on acceptor doping (Fig. 6B) confirms that the p-type electronic conduction is dominant compared to n-type.

The Seebeck coefficient of pure $CeVO_{4+\delta}$ is positive (Fig. 6C), in agreement with literature [5,7]. Doping with calcium and strontium leads to a change in the sign of thermo-e.m.f.; the type of temperature dependencies of the electrical properties remains, however, similar to that of undoped cerium orthovanadate. The Jonker-type analysis [17] of these data shows that such a behavior results from increasing hole concentration and cannot be attributed to a transition from p- to n-type conduction. In particular, all $\alpha - \ln(\sigma)$ isotherms presenting the data points with different calcium content have a negative slope comparable to –k/e (Fig. 7). Taking into account literature data [18] showing that electronic conduction in both cerium and vanadium oxides occurs via hopping mechanisms, small polaron conduction in $Ce_{1-x}A_xVO_{4+\delta}$ was assumed. For a hopping mechanism, the Seebeck coefficient (α) can be expressed as [17-19]

$$\alpha = \frac{k}{e}\left[\ln\left(\frac{N-\beta p}{p}\right) + \frac{q}{k\cdot T}\right] \qquad (5)$$

where p is the hole concentration, N is the total concentration of sites participating in the conduction process, q is the transported heat of the holes, and β is the blocking factor, which renders a fraction of the sites neighbouring a charge carrier unavailable for occupancy. The transported heat, q, which can be estimated from the temperature dependencies of thermopower at fixed carrier concentration, is often neglected [19]. Evaluation of p/N ratio by eq. (5) shows that more than a half of sites, available for hopping in the lattice of $Ce_{1-x}A_xVO_{4+\delta}$, should be occupied; the p/N ratio increasing from 0.61 (x = 0) up to 0.91 (x = 0.2) in air. As the transported heat of the holes is positive by definition, it may compensate the negative concentration-dependent part of eq. (5), thus retaining positive values of Seebeck coefficient of $CeVO_{4+\delta}$. Increasing calcium content leads to a greater p/N ratio and, hence, lower Seebeck coefficient, which becomes negative at $x \geq 0.1$. At the same time, the dominant oxidation state of vanadium in these conditions is 5+ [8], and V^{5+} cations in vanadates contribute, as a rule, to n-type electronic transport [5]. Thus, cerium sublattice is supposed to provide the electron-hole conduction. This assumption is supported by the decrease in the tetragonal unit cell parameters on doping (inset in Fig. 2A), suggesting the presence of Ce^{4+} cations since the ionic radius of 8-coordinated cations increases as $Ce^{4+} < Ce^{3+} \approx Ca^{2+} < Sr^{2+}$. However, occurrence of high fractions of tetravalent ceria (60-90%) would contradict the XAS and TGA data [7,9]. Therefore, a significant part of cerium sites is probably blocked and is not available for the electron-hole hopping, probably due to local distortion of the lattice near Ce^{4+} cations having relatively small size.

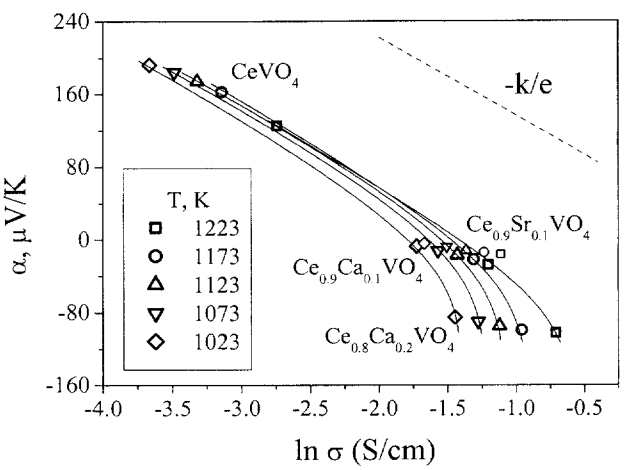

Fig. 7. Seebeck coefficient of $Ce_{1-x}A_xVO_{4+\delta}$ in air, plotted vs. corresponding conductivity values.

4. Conclusions

Dense single-phase ceramics of zircon-type $Ce_{1-x}A_xVO_4$ (A = Ca, Sr; x = 0 – 0.2) were studied using XRD, SEM/EDS, and the measurements of total electrical conductivity, faradaic efficiency and Seebeck coefficient at 973-1223 K in air. Substitution of cerium with alkaline-earth cations leads to a higher p-type electronic conductivity and to lower Seebeck coefficient, which changes the sign from positive to negative due to increasing electron-hole concentration. The oxygen ion transference numbers of $Ce(A)VO_{4+\delta}$ in air, determined from the faradaic efficiency data, vary in the range from 2×10^{-4} to 6×10^{-3} at 973-1223 K, increasing with temperature and decreasing when alkaline-earth dopant concentration increases. The ionic conductivity of $Ce_{1-x}A_xVO_{4+\delta}$ is essentially independent of composition, indicating an interstitial ion migration mechanism. This suggests that the cerium vanadate-based phases are oxygen hyperstoichiometric, in agreement with estimates of the electron-hole concentration. The activation energies for p-type electronic and oxygen ionic conductivities are 39-45 kJ/mol and 87-112 kJ/mol, respectively.

5. Acknowledgements

This research was partially supported by the FCT, Portugal (PRAXIS and POCTI programs and project BD/6827/2001), the Belarus Ministry of Education and Science, and the Commission of the Russian Academy of Sciences for Young Scientists Support (6th competition, grant 192).

6. References

[1] U.O. Krasovec, B. Orel and R. Reisfeld, Electrochem. Solid State Lett. **1**, 104 (1998).

[2] A.M. Salvi, F. Decker, F. Varsano and G. Speranza, Surf. Interface Anal. **31**, 255 (2001).

[3] R. Cousin, D. Courcot, E. Aad Abi, S. Capelle, J.P. Amoureux, M. Dourbin, M. Guelton and A. Aboukais, Colloid. Surface A **158**, 43 (1999).

[4] J. Matta, D. Courcot, E. Aad Abi and A. Aboukais, in: Environment and Solar, Proc. 2000 Mediterranean Conf., IEEE, Piscataway, NJ, 2001, p. 278.

[5] K. Gaur and H.B. Lal, J. Mater. Sci. **20**, 3167 (1985).

[6] H.C. Nguyen and J.B. Goodenough, J. Solid State Chem. **119**, 24 (1995).

[7] A. Watanabe, J. Solid State Chem. **153**, 174 (2000).

[8] T. Hirata and A. Watanabe, J. Solid State Chem. **158**, 254 (2001).

[9] R.F. Reidy and K.E. Swider, J. Am. Ceram. Soc. **78**, 1121 (1995).

[10] V.V. Kharton, A.P. Viskup, F.M. Figueiredo, E.N. Naumovich, A.A. Yaremchenko and F.M.B. Marques, Electrochim. Acta **46**, 2879 (2001).

[11] V.V. Kharton, A.P. Viskup, A.V. Kovalevsky, F.M. Figueiredo, J.R. Jurado, A.A. Yaremchenko, E.N. Naumovich and J.R. Frade, J. Mater. Chem. **10**, 1161 (2000).

[12] V.V. Kharton, A.P. Viskup, A.V. Kovalevsky, F.M. Figueiredo, J.R. Jurado, A.A. Yaremchenko, E.N. Naumovich and J.R. Frade, J. Mater. Chem. **10**, 1161 (2000).

[13] E.B. Mitberg, M.V. Patrakeev, A.A. Lakhtin, I.A. Leonidov, V.L. Kozhevnikov and K.R. Poeppelmeier, J. Alloy. Compd. **274**, 103 (1998).

[14] D.P. Fagg, J.C. Waerenborgh, V.V. Kharton and J.R. Frade, Solid State Ionics **146**, 87 (2002).

[15] E.V. Tsipis, M.V. Patrakeev, V.V. Kharton, N.P. Vyshatko and J.R. Frade, J. Mater. Chem., accepted for publication (2002).

[16] V.V. Kharton, A.P. Viskup, A.V. Kovalevsky, E.N. Naumovich and F.M.B. Marques, Solid State Ionics **143**, 337 (2001).

[17] G.H. Jonker, Philips Res. Rep. **23**, 131 (1968).

[18] P. Kofstad, Nonstoichiometry, Diffusion and Electrical Conductivity in Binary Metal Oxides, Wiley-Interscience, New York, 1972.

[19] K. Kobayashi, S. Yamaguchi, T. Tsunoda and Y. Imai, Solid State Ionics **144**, 123 (2001).

Paper presented at the 9th EuroConference on Ionics, Ixia, Rhodes, Greece, Sept. 15 – 21, 2002.

Manuscript rec. Sept. 16, 2002; acc. Mar. 10, 2003.